

## High-Throughput Screen in *Cryptococcus neoformans* Identifies a Novel Molecular Scaffold That Inhibits Cell Wall Integrity Pathway Signaling

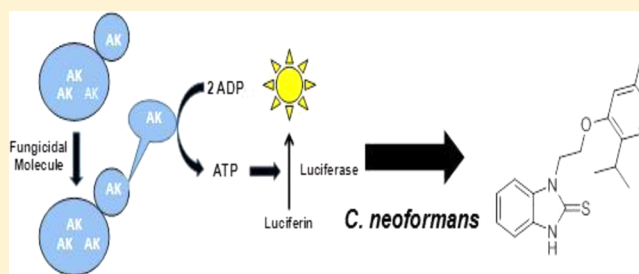
Kate Hartland,<sup>†</sup> Jun Pu,<sup>†</sup> Michelle Palmer,<sup>†</sup> Sivaraman Dandapani,<sup>†</sup> Philip N. Moquist,<sup>†</sup> Benito Munoz,<sup>†</sup> Louis DiDone,<sup>§</sup> Stuart L. Schreiber,<sup>†</sup> and Damian J. Krysan<sup>\*,§,⊗</sup>

<sup>†</sup>Center for the Science of Therapeutics, Broad Institute of Harvard and MIT, 7 Cambridge Center, Cambridge, Massachusetts 02142, United States

<sup>§</sup>Department of Pediatrics and <sup>⊗</sup>Department of Microbiology/Immunology, University of Rochester School of Medicine and Dentistry, 601 Elmwood Avenue, Rochester, New York 14642, United States

**ABSTRACT:** *Cryptococcus neoformans* is one of the most important human fungal pathogens; however, no new therapies have been developed in over 50 years. Fungicidal activity is crucially important for an effective anticryptococcal agent and, therefore, we screened 361,675 molecules against *C. neoformans* using an adenylate kinase release assay that specifically detects fungicidal activity. A set of secondary assays narrowed the set of hits to molecules that interfere with fungal cell wall integrity and identified three benzothioureas with low in vitro mammalian toxicity and good in vitro anticryptococcal (minimum inhibitory concentration = 4  $\mu\text{g}/\text{mL}$ ). This scaffold inhibits signaling through the cell wall integrity MAP kinase cascade. Structure–activity studies indicate that the thiocarbonyl moiety is crucial for activity. Genetic and biochemical data suggest that benzothioureas inhibit signaling upstream of the kinase cascade. Thus, the benzothioureas appear to be a promising new scaffold for further exploration in the search for new anticryptococcal agents.

**KEYWORDS:** *Cryptococcus neoformans*, antifungal, cell wall integrity pathway, high-throughput screening, yeast cell wall, mitogen-activated protein kinase



Invasive fungal infections are an important cause of morbidity and mortality, particularly in people living with compromised immunity.<sup>1</sup> Of the specific fungal infections that affect humans, cryptococcosis plays a prominent role in global health because of its high incidence in people infected with HIV.<sup>2</sup> Recent epidemiologic studies estimate that up to 1 million new cases of cryptococcosis occur each year and that approximately 600,000 people die each year.<sup>3</sup> Although the vast majority of these cases are associated with HIV/AIDS and are due to *Cryptococcus neoformans*, an ongoing outbreak of cryptococcosis due to *Cryptococcus gattii* has involved apparently immunocompetent patients as well.<sup>4</sup> Cryptococcosis typically presents as either meningoencephalitis or, less commonly, pneumonia.<sup>2</sup> Patients with previously undiagnosed HIV are frequently identified after they present with symptoms of cryptococcal meningoencephalitis (CEM). As such, many patients must first survive CEM if they are to take advantage of the dramatic advances in the treatment of HIV.<sup>5</sup>

Currently, the gold standard treatment for CEM is amphotericin B combined with flucytosine. A landmark clinical trial has established the combination is more effective than amphotericin B alone.<sup>6</sup> This therapy, however, has a number of shortcomings: (1) both agents are toxic and require close laboratory monitoring of the patients; (2) amphotericin B must

be administered intravenously and, thus, requires medical infrastructure that is not available in many resource-limited regions with high HIV prevalence; and (3) flucytosine is expensive and not readily available in resource-limited regions. As a result of these issues, many patients in resource-limited regions are treated with fluconazole, a safe, orally administered agent that is cheap and/or available by donation. Unfortunately, fluconazole is less effective than amphotericin B, and patients treated with fluconazole alone have a much higher rate of mortality.<sup>7</sup> The lower efficacy of fluconazole is due, at least in part, to the fact that it is fungistatic, whereas amphotericin B/flucytosine is fungicidal.<sup>6,7</sup> As a result, amphotericin B/flucytosine treatment leads to a reasonably rapid clearance of *Cryptococcus* from the cerebrospinal fluid, whereas fluconazole does not. Clearance of the pathogen from the cerebrospinal fluid, also known as the early fungicidal activity, correlates with patient outcome.<sup>7</sup> When these issues and observations are taken together, it seems clear that new, widely available, orally administered fungicidal agents are needed for the treatment of cryptococcosis.<sup>8</sup> As a result, we and others have explored

Received: September 25, 2015

Published: November 6, 2015

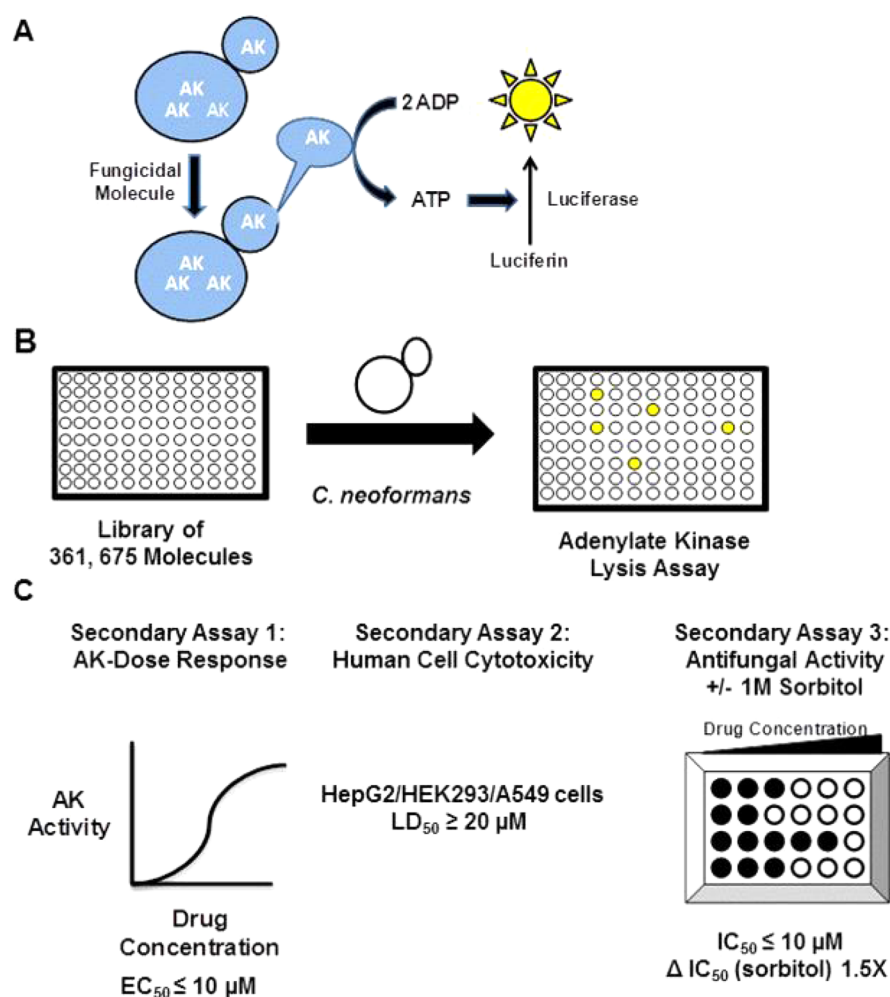


**Figure 1.** Screening strategy. (A) Schematic of adenylate kinase (AK) release assay as a reporter of fungal cell lysis. Fungicidal molecule disrupts cell integrity, leading to release of the intracellular enzyme AK into the growth medium. The activity of AK is determined by coupling the conversion of ADP to ATP, which, in turn, drives luciferase activity. (B) Primary screen in *C. neoformans*. (C) Set of three secondary assays and criteria.

approaches to directly identify molecules with fungicidal activity against *C. neoformans*.<sup>9–11</sup>

The pace of new antifungal drug development has been extremely slow.<sup>8</sup> The current gold standard for cryptococcosis is based on drugs identified in the late 1950s and early 1960s.<sup>12</sup> The most recently developed class of clinically used antifungal drugs is the echinocandins; they were identified in the early 1970s and were introduced to clinical practice in 2002 with the launch of caspofungin. The echinocandins are an extremely useful class of molecules that inhibit 1,3- $\beta$ -glucan synthesis in a wide range of clinically relevant fungi. The integrity of the fungal cell wall is crucially dependent on 1,3- $\beta$ -glucan. Because human cells lack this structure, the fungal cell wall has long been regarded as a nearly ideal antifungal drug target; by analogy, antibiotics that target the bacterial cell wall include penicillins, cephalosporins, and glycopeptides and are the lynchpins of current therapy. Molecules that disrupt the fungal cell wall generally lead to cell lysis and, thus, for the majority of species, are fungicidal. For *Cryptococcus*, however, the echinocandins have very poor activity and are clinically not useful.<sup>2</sup> The echinocandins inhibit *C. neoformans* 1,3- $\beta$ -glucan synthesis in vitro; the reason for the lack of efficacy is not clear.<sup>13</sup> Interestingly, nikkomycin Z is the other cell wall-targeted molecule that has been extensively studied as a

potential antifungal drug, and *C. neoformans* is also resistant to it, whereas most other pathogens are susceptible.<sup>14</sup> Thus, the cell wall of *C. neoformans* appears to have features that distinguish it from other pathogenic fungi, particularly with respect to susceptibility to cell wall-targeted antifungal drugs.<sup>15</sup>

The vast majority of small-molecule screens for agents with biological activity against yeast have been carried out in the ascomycetous yeasts such as *Saccharomyces cerevisiae* and *Candida albicans*. To our knowledge, relatively few screens have been performed in the basidiomycetous yeast *C. neoformans*, a species that has diverged significantly from the ascomycetes.<sup>16</sup> This divergence would be expected to lead to significant distinctions in the functions of pathways and processes in species.<sup>17</sup> Consistent with that assertion, the first large-scale chemical genetic screen of *C. neoformans* found that the chemical–genetic responses were distinct from those observed with *S. cerevisiae*.<sup>18</sup> Similarly, our screening efforts have shown that molecules frequently have very different activities between *C. neoformans* and either *S. cerevisiae* or *Candida albicans*.<sup>16</sup> On the basis of these considerations, it seemed apparent that the best approach to identifying molecules with activity toward *C. neoformans* would be to directly screen that organism.

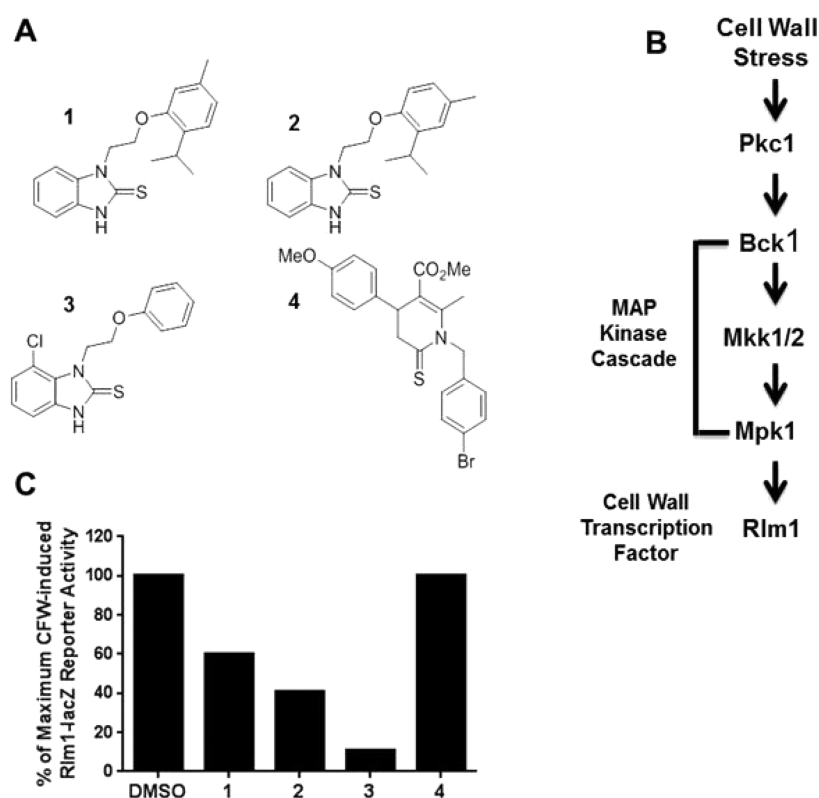


**Figure 2.** Benzothiourea class of molecules inhibits cell wall integrity signaling cascade. (A) Molecules 1–4 were identified in the primary and secondary screens. (B) A schematic of the cell wall integrity pathway (CWIP) shows MAP kinase cascade conserved throughout yeast. (C) Molecules 1–3 but not 4 (20  $\mu\text{M}$ ) inhibit Calcofluor white (CFW) mediated activation of the Rlm1-*lacZ* reporter of CWIP activity in *S. cerevisiae*. The bars represent the mean of three replicates with SD <10%.

We were interested in identifying molecules with activity toward cell wall-related processes in *C. neoformans*. We hypothesized that these molecules would not only represent potential antifungal drug candidates but could also function as molecular probes of *C. neoformans* cell wall biology. To identify cell wall-targeted small molecules, we took advantage of an assay developed in our laboratory that uses the extracellular release of the intracellular enzyme adenylate kinase as a reporter of cell lysis in *C. neoformans*.<sup>9</sup> As alluded to above, cell lysis is the terminal phenotype of yeast cells with damaged cell walls; however, cell lysis is not specific to cell wall damage and can also result from membrane damage. Therefore, we used a set of secondary screening assays designed to select for cell wall active molecules. These assays were (1) osmotic suppression of antifungal activity<sup>19</sup> and (2) modulation of a cell wall stress reporter strain.<sup>20</sup>

As described below, a high-throughput screen was carried out as part of the NIH Molecular Libraries Initiative<sup>21</sup> and led to the identification of a set of benzothioureas that (1) have good *in vitro* activity against *C. neoformans*, (2) have low toxicity toward human cell lines, and (3) inhibit signaling through the cell wall integrity MAP kinase pathway in *C. neoformans*.

## RESULTS AND DISCUSSION

**Screening Strategy.** To identify a set of molecules enriched for those that target cell wall-related processes in *C. neoformans*, we designed the screening strategy outlined in Figure 1. The primary screen was for molecules that cause release of the intracellular enzyme adenylate kinase (AK) into the culture medium using *C. neoformans* var. *grubii* strain

H99.<sup>9,16</sup> The release of AK activity is a reporter of fungal cell lysis and is an extremely sensitive marker of antifungal activity (Figure 1A). Previous studies in our laboratory have shown that it is more sensitive than growth-based assays for some classes of molecules.<sup>22</sup> This is because up to 30% of the cells in a culture can undergo lysis without affecting the final density of the culture, the most convenient readout for high-throughput growth assays. As mentioned above, cell lysis is the hallmark phenotype of fungal cells with compromised cell wall integrity and, thus, the AK assay is a sensitive approach to identifying molecules that target the cell wall. It is important to note that fungistatic agents such as fluconazole cause no increase in AK activity as compared to solvent controls.<sup>22</sup>

AK release for each hit was confirmed using an eight-point dose–response experiment, and molecules with an effective concentration ( $\text{EC}_{50}$ ) <10  $\mu\text{M}$  were advanced for further evaluation (Figure 1C). Molecules were then screened against three mammalian cell lines (HepG2, HEK293, and A549), and molecules that showed toxicity at concentrations <20  $\mu\text{M}$  were removed from further testing (Figure 1C). The antifungal activity of the molecules toward *C. neoformans* was determined using a microtiter plate-based Alamar blue viability assay in the presence and absence of 1 M sorbitol. Sorbitol provides osmotic stabilization for cells that have defective cell walls.<sup>19</sup> For example, *C. neoformans* mutants lacking Mpk1, the terminal MAP kinase of the cell wall integrity pathway (CWIP), undergo lysis when cultivated at 37 °C in standard media because growth at this temperature causes cell wall stress.<sup>23</sup> However, in the presence of 1 M sorbitol, *mpk1* $\Delta$  is able to grow at 37 °C.<sup>23</sup> Sorbitol-remedial growth defects have been widely used in the

characterization of yeast mutants with cell wall defects.<sup>19,20,23</sup> Therefore, we used sorbitol suppression as a convenient screen to identify molecules with increased likelihood of targeting the cell wall. It is important to note that sorbitol is also a cell stressor, and cells lacking a functional hyperosmotic-glycerol (HOG) MAP kinase pathway are unable to grow in the presence of sorbitol.<sup>24</sup> Thus, this assay removes molecules that may cause lysis due to interfering with the HOG pathway or other components of the cellular response to high osmotic stress. Molecules with an inhibitory concentration ( $IC_{50}$ ) in media lacking sorbitol  $<10 \mu\text{M}$  and an increase in  $IC_{50}$  of  $>1.5$ -fold in the presence of sorbitol were advanced (Figure 1C).

Finally, we examined the effect of candidate hits on the activation of a *S. cerevisiae*-based cell wall integrity pathway reporter strain. The *S. cerevisiae* strain used for this assay was CRY2, which is derived from the W303 background. The strain harbored a plasmid containing a  $\beta$ -galactosidase (*lacZ*) gene under the control of two copies of the consensus Rlm1p transcription factor binding sites. Rlm1p is activated by the cell wall integrity MAP kinase signaling cascade<sup>20</sup> and regulates a large number of cell wall-stress related genes (Figure 2B). Molecules interfering with cell wall-related processes could affect activation of the reporter in one of two ways. First, the molecule could perturb the cell wall directly or interfere with cell wall biosynthesis, leading to activation of the CWIP. Second, the molecule could decrease signaling through the CWIP. CWIP activity is required during the cell cycle to regulate the cell wall remodeling that occurs during the budding process and, as discussed above, is required for *C. neoformans* and *S. cerevisiae* growth at 37 °C.<sup>20,23</sup> Therefore, we performed two assays to test these potential effects. First, we examined the ability of the molecules to directly activate the reporter and, second, we determined the effect of the molecule on the ability of Calcofluor white, a chitin-binding molecule that induces cell wall stress, to activate the CWI pathway. We have previously shown that molecules which inhibit activation of the CWIP prevent CFW-induced activation of the *Rlm1-lacZ* reporter.<sup>25</sup> A *S. cerevisiae*-based CWIP reporter was used in the strategy as an expedient method to narrow the set of hits to those affecting cell wall-related processes. A limitation to this approach is that molecules that may affect *C. neoformans* cell wall integrity through processes that are not conserved with *S. cerevisiae* are likely to be missed. The primary goal of the screen was to find molecules that are active against *C. neoformans* and not to find molecules active only against *C. neoformans*. The data set generated by the primary screen may contain the latter molecules, but additional analysis will be required to identify those molecules.

**Adenylate Kinase-Based Screen Identifies Molecules with Fungicidal Activity toward *C. neoformans*.** A total of 361,675 molecules were screened at the Broad Institute using the AK assay in 1536-well format. As more completely detailed under Methods, *C. neoformans* strain H99 was cultivated overnight to exponential phase ( $OD_{600} < 1$ ), harvested, washed with fresh medium, and resuspended (cell density of  $5 \times 10^6$  cells/mL) in a 1536-well plate that had previously been charged with test compounds by pinning. The plates were incubated at 37 °C for 4 h before the addition of AK detection reagent (ToxiLight). The luminescence was then determined after an additional 30 min of incubation. The intrascreening  $Z'$  scores were between 0.5 and 0.8 for the majority of plates. Each plate contained clomiphene as a positive control; clomiphene is a triphenylethylene estrogen receptor antagonist that induces cell

lysis and strong AK signal in *C. neoformans*,<sup>16</sup> and molecules inducing AK release that was at least 80% of that induced by the positive control were called “hits”.

An initial set of 737 molecules were identified from the primary screen for a hit rate of 0.2%. The entire set of primary and secondary screening data are available on PubChem (BioAssay AID: 651665; for a complete listing of AID numbers for the individual assays, please see Methods). This set of 737 molecules along with 306 structurally related analogues (total number = 1043 compounds) was retested using the AK assay, and 71 showed a smooth dose–response curve with an  $EC_{50}$  concentration of  $<10 \mu\text{M}$ . The cytotoxicity of this set was screened against three cell lines (HepG2, HEK293, and A549) using the Cell Titer Glo Assay (Promega). Only three molecules were cytotoxic below  $20 \mu\text{M}$  and, thus, 68 molecules met criteria for advancement. Interestingly, 63 of the 71 molecules were thiourea derivatives. Many of the cyclic thiourea-containing hits were highly related and, therefore, the set was reduced in number by eliminating molecules with potentially problematic functional groups. Through this process a subset of 32 molecules were selected for evaluation for cell wall activity using the sorbitol suppression and cell wall stress reporter secondary assays.

The anticryptococcal activity of the molecules was determined using the well-established Alamar blue viability assay adapted for yeast cells in 384-well format in synthetic complete medium alone or supplemented with 1 M sorbitol. Of the set of 32 hits, 10 inhibited *C. neoformans* growth with  $IC_{50} <10 \mu\text{M}$ ; 15 had  $IC_{50}$  values  $>10 \mu\text{M}$ ; and 7 were judged inactive ( $IC_{50} > 50 \mu\text{M}$ ). The ability of the molecule to inhibit *C. neoformans* in synthetic media was then compared to its activity in medium supplemented with 1.0 M sorbitol. Only four compounds showed a  $>1.5$ -fold increase in  $IC_{50}$  upon addition of sorbitol to the culture medium (Figure 2A). Thus, the majority of the molecules identified in our screen appear to cause lysis through non-cell-wall-related mechanisms.

Although a number of mechanisms could account for this activity, previous AK-based screens of *C. neoformans* as well as other yeasts indicate that the most commonly identified class of molecules comprises those that directly target the plasma membrane. The ability of sorbitol to suppress the antifungal activity of a molecule is not entirely specific to cell wall-targeted molecules. However, molecules that have sorbitol-independent antifungal activity are much less likely to be cell wall-targeted. Of the four molecules that showed sorbitol-suppressible anticryptococcal activity, all four were cyclic thiocarbonyl-based structures (Figure 2A). Three were thioureas (compounds 1, 2, and 3), and one was a thio-amide derivative (4). The set of primary hits contained numerous molecules related to 4; however, 4 was the only molecule that showed sorbitol suppression. We also determined the antifungal activity of these molecules using the CLSI standardized minimum inhibitory concentration (MIC) assay.<sup>26</sup> The benzothioureas had similar MICs (4–8  $\mu\text{g}/\text{mL}$ ), whereas the six-membered ring molecule was significantly less active (MIC = 32  $\mu\text{g}/\text{mL}$ ). As a reference, the MIC for fluconazole is generally between 2 and 8  $\mu\text{g}/\text{mL}$  for *C. neoformans* strains. Thus, the primary screen provided two candidate scaffolds with potential cell wall-targeted anticryptococcal activity.

**A Novel Benzothiourea Scaffold Inhibits Activation of the Cell Wall Integrity Pathway in *C. neoformans*.** To evaluate the cell wall-associated activity of the four candidate molecules, we used a reporter of cell wall integrity pathway

(CWIP) activity. As outlined in Figure 2B, the CWIP is a MAP kinase signaling cascade that is regulated by protein kinase C, which is, in turn, dependent on a number of upstream proteins.<sup>20</sup> The pathway is highly conserved across fungal species including *C. neoformans* and *S. cerevisiae*.<sup>15,20,23</sup> Cell wall damage and stress caused by growth at 37 °C, small molecules, cell wall-degrading enzymes, and oxidative damage as well as a number of other stressors lead to activation of the pathway.<sup>20</sup> The MAP kinase cascade ends with the phosphorylation of Mpk1 (also called Slk2). Activated Mpk1 modulates the activity of a number of transcription factors including Rlm1, which orchestrate a transcriptional program to compensate for the damage to the cell wall.<sup>20</sup> Genes up-regulated by the CWIP include those for cell wall biosynthesis (e.g., 1,3- $\beta$ -glucan synthase (*FKS2*) and chitin synthase (*CHS3*)), cell wall-remodeling proteins (e.g., glucosyl transferases (*CRH2*)), and a plethora of cell wall mannoproteins that appear to play a structural role.<sup>20</sup> During normal yeast physiology, the activity of the CWIP is also tied to the cell cycle and is activated as part of the transition to stationary phase upon nutrient depletion.<sup>27</sup>

We transformed *S. cerevisiae* strain CRY2 with a plasmid containing two copies of the consensus Rlm1p-binding sites fused to a  $\beta$ -galactosidase gene [*CRY2* (*2XpRLM1-lacZ*)]. This reporter was developed by the Levin laboratory and is a widely used reporter of CWIP activation.<sup>28</sup> Molecules, condition, or mutations that cause cell wall stress lead to increased expression of Rlm1 targets and, hence, increased  $\beta$ -galactosidase activity.<sup>24</sup> For example, exposure of *S. cerevisiae* cells harboring this plasmid to the chitin binding agent Calcofluor white leads to a 5-fold increase in  $\beta$ -galactosidase activity. *CRY2* (*2XpRLM1-lacZ*) was exposed to a dilution series of the four candidates along with a subset of the 32 initial hits. None of the molecules triggered the CWIP reporter and, thus, did not appear to cause a cell wall stress response in *S. cerevisiae* (data not shown); however, it is possible that some of the molecules may cause cell wall stress in *C. neoformans* in a manner that is not conserved in *S. cerevisiae*.

The candidate molecules could also disrupt the cell wall by interfering with CWIP activation either by inhibiting the components of the pathway or by preventing upstream regulators from interacting with the pathway. To test this possibility, we exposed *CRY2* (*RLM1-lacZ*) cells to Calcofluor white in the presence of the candidate molecules and compared the resulting  $\beta$ -galactosidase signal to solvent-treated cells. All three of the benzothioureas (**1**, **2**, and **3**) inhibited Calcofluor white-mediated CWIP activation (Figure 2C), whereas the six-membered ring thioamide **4** had no effect up to concentrations of 20  $\mu$ M. To rule out the possibility that the decreased activity was due to the toxic effect of the molecules on the cell, we determined the MIC for the three benzothioureas toward *CRY2* (*RLM1-lacZ*) under the assay conditions; the MIC for all three molecules was >40  $\mu$ M. These data indicate that the benzothiourea scaffold inhibits CWIP activation and, given the effect of sorbitol on its anticryptococcal activity, this inhibition appears to contribute to its mechanism of action.

To further confirm that the benzothioureas interfere with signaling through the CWIP pathway, we examined the effect of the molecules on the Calcofluor white-induced phosphorylation of Mpk1, the terminal MAPK of the CWIP (Figure 2B). Exponential phase *C. neoformans* cells with a *MPK1* allele containing a fusion to the FLAG epitope tag were exposed to solvent,<sup>29</sup> compound **3**, Calcofluor white, or a combination of **3** and Calcofluor white. Western blotting of extracts from these

cells with an antibody specific for the phosphorylated form of Mpk1 indicated that, as expected, Calcofluor white induced phosphorylation of Mpk1. Consistent with the results obtained with the CWIP reporter, treatment with **3** reduced Calcofluor white-mediated Mpk1 phosphorylation but did not trigger activation by itself (Figure 3A). As shown in Figure 3B, similar

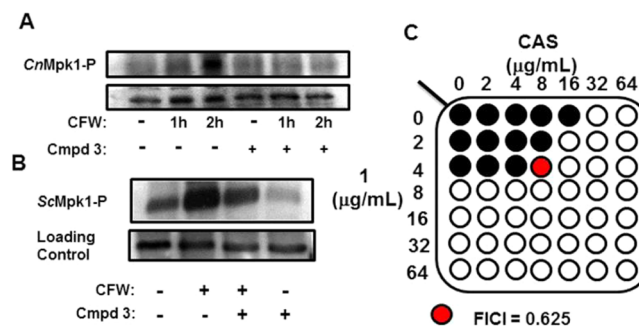


**Figure 3.** Benzothioureas inhibit phosphorylation of Mpk1 and are additive with the cell wall-targeted antifungal caspofungin. (A) *C. neoformans* containing an allele of Mpk1 tagged with FLAG epitope was exposed to CFW (20  $\mu$ g/mL)  $\pm$  compound **3** (20  $\mu$ M) for the indicated time periods and compared to DMSO (1%)-treated cells by Western blotting with an antibody specific for phosphorylated form of MAPK. The samples were also probed with an anti-FLAG antibody. (B) *S. cerevisiae* BY471 cells were processed as in (A) except that Mpk1 was not epitope-tagged and the loading control was a nonspecific band present in all samples. (C) A schematic of the checkerboard assay probing the interaction of **1** with caspofungin against *C. neoformans* H99 cells is shown. Black wells indicate growth; white wells indicate no growth; the red well indicates the lowest concentrations of **1** and caspofungin inhibiting growth. FICI, fractional inhibitory concentration index.

results were obtained with *S. cerevisiae*, indicating that the molecule interferes with CWIP signaling in both species. Interestingly, treatment with **3** alone reduces the constitutive Mpk1 phosphorylation that accompanies exponential phase growth.<sup>27</sup> Taken together, these data indicate that the benzothiourea scaffold interferes with CWIP signaling.

We hypothesized that inhibition of the CWIP by benzothiourea would lead to a positive interaction of the molecule with other cell wall-targeted drugs. As mentioned above, echinocandins such as caspofungin inhibit 1,3- $\beta$ -glucan synthesis in *C. neoformans*, but the concentrations of drug required to inhibit growth with these drugs are too high to be clinically useful. However, caspofungin causes cell wall damage to *C. neoformans* and, as reported by Kraus et al., triggers phosphorylation of Mpk1.<sup>23</sup> We, therefore, tested the interaction between caspofungin and **1** by standard checkerboard assays. Consistent with this model, subinhibitory concentrations of **1** reduced the concentration of caspofungin needed to inhibit *C. neoformans* 8-fold (Figure 3C). The fractional inhibitory concentration index for this interaction is additive (0.625) because the concentration of compound **1** is 2-fold below the MIC. However, this provides additional support for the fact that compound **1** inhibits CWIP signaling in *C. neoformans* and that this inhibition contributes to its mechanism of antifungal activity. Previous studies with other fungal pathogens such as *Aspergillus fumigatus* have shown that inhibitors of the CWIP such as the PKC inhibitor staurosporine are additive or synergistic with caspofungin.<sup>30</sup> The additive interaction between **1** and caspofungin further supports the

notion that the molecule is targeting the CWIP as part of its mechanism of action. Thus, the AK screening approach was successful in identifying molecules that target cell wall-related processes in *C. neoformans*.

**Structure–Activity Analysis Indicates the Thiourea Moiety Is Crucial for Anticryptococcal Activity of the Benzothiourea Scaffold.** None of the four benzothioureas showed significant toxicity in three different cell lines, and molecule **1** was nontoxic up to 80  $\mu\text{M}$  against HEK293 cells (higher concentrations were not tested); thus, the ratio of MIC to  $\text{LD}_{50}$  is  $\geq 3$ . Subsequent characterization focused on compound **1** on the basis of its low toxicity. The thiourea moiety of the scaffold could exist as one of two tautomers: (1) thiourea or (2) thioimidazole. Literature data suggest that these compounds exist as the thiourea tautomer, predominantly. Consistent with these data, compound **1** shows a very strong C=S stretching band in the infrared spectra (IR) at  $1256\text{ cm}^{-1}$ . In addition, a strong band is present at  $1500\text{--}1510\text{ cm}^{-1}$ , indicative of a  $\text{--RNC(=S)--NH--}$  system. Importantly, both the  $^1\text{H}$  and  $^{13}\text{C}$  nuclear magnetic resonance (NMR) spectra show a single species, indicating that the thiourea is the only detectable tautomer. In addition, compound **1** is stable in human and mouse plasma with 100% remaining intact after 5 h of incubation. A number of clinically used drugs contain the thiourea moiety including the thyroid medication propylthiouracil and the antituberculosis drugs isoxyl and thiacetazone. Thiourea-containing drugs are associated with neutropenia and agranulocytopenia. This adverse event is relatively rare, usually reversible, and associated with long-term use. Although this potential liability does not preclude the development of thiourea-containing medications, avoiding this functional group would be ideal if possible. Therefore, our initial structure–activity analysis of the thiourea scaffold of anticryptococcal agents focused on evaluating the role of the thiourea moiety as one of its primary goals.

A total of 60 molecules structurally related to the 3 initial benzothiourea hits were either synthesized or purchased from commercial vendors. The majority of analogues were generated by the synthetic sequence shown in Figure 4. These derivatives

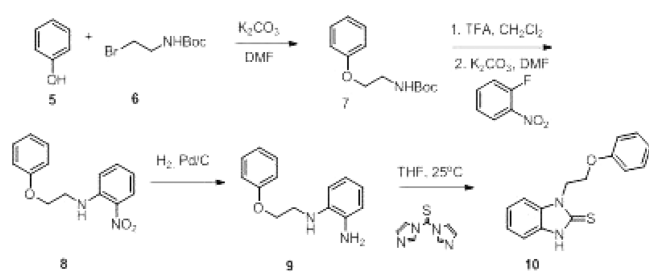


**Figure 4.** General scheme for the synthesis of benzothioureas.

were evaluated using the AK assay, HEK293 toxicity, and the sorbitol/no sorbitol antifungal activity assay. From this set, a total of 19 molecules were selected for CLSI MIC testing. The complete biological testing data for the entire set are available at PubChem (PubChem AIDs 651665). Overall, this initial SAR did not lead to the synthesis of any analogues that had improved activity relative to compounds **1** and **3**. Therefore, we present antifungal data for selected examples that illustrate the general trends that emerged from the SAR.

As shown in Figure 5, the parent phenoxy-substituted benzothiourea (**10**) is approximately 2-fold less active than

compound **1** or **2** and 4-fold less active than compound **3**. Replacement of the thiocarbonyl group of **5** with a carbonyl (**11**) led to an inactive molecule as did conversion of the thiourea to an imidazole (**12**). Additionally, replacement of the thiourea with standard bioisosteres such as guanidinium or *N*-cyano-guanidinium<sup>31</sup> led to unstable or inactive molecules (not shown). These results indicate that the thiocarbonyl group plays an important role in the activity of this scaffold and also suggest that the thiocarbonyl tautomer may be crucial. The latter notion is supported by the fact that the *S*-alkylated derivative **13** is 4-fold less active than the thiocarbonyl parent (**1**). Introduction of methyl (**14**) and chloro (**15**) substituents at the para-position of the phenoxy improved activity modestly (2-fold) relative to molecule **10**; the *p*-ethoxy analogue **16**, however, showed the same activity as **10**. As noted above, the most active derivative contains a chloro atom at the 3-position of the benzothiourea ring (**3**). Placement of the 6-fluoro group on the benzothiourea ring (**17**) decreased activity 2-fold, whereas a methyl substituent at the 5-position (**18**) had no effect relative to compound **10**. Overall, the initial SAR revealed that the thiourea is critical for activity and established regions of the scaffold that affect activity. However, these studies did not yield an improvement in activity relative to the initial hits.

**Anticryptococcal Activity of the Benzothiourea Scaffold Correlates with Cell Wall Integrity Pathway Inhibition but Other Targets Contribute to Mechanism of Action.** We selected a set of six analogues with a range of MIC values from 4 to 32  $\mu\text{g}/\text{mL}$  and examined their effect on CFW-induced Mpk1 phosphorylation. As described above, *C. neoformans* cells were treated with CFW in the presence or absence of the benzothiourea molecule and processed for Mpk1-P by Western blot. The effect of each molecule was quantitated by densitometry relative to CFW-only treated cells and then plotted to determine if Mpk1 phosphorylation correlated with anticryptococcal activity. As shown in Figure 6A, the correlation between MIC and Mpk1 inhibition was reasonable. The most active molecule in both assays was **3**, with an MIC of 4  $\mu\text{g}/\text{mL}$  and a 90% inhibition of Mpk1 phosphorylation. Although the range of MICs is only 8-fold, these data are consistent with CWIP inhibition contributing to the anticryptococcal activity of the benzothiourea scaffold.

The only component of the CWIP MAP kinase cascade<sup>20</sup> that is essential in *C. neoformans* is protein kinase C 1 (Pkc1). Therefore, we tested the effect of **1** on the protein kinase C activity of *C. neoformans* cell lysates using a fluorescent Pkc1 specific substrate as previously described.<sup>29</sup> Under assay conditions in which we could detect a 25% reduction in Pkc1 activity using the protein kinase C inhibitor staurosporine (data not shown), benzothiourea **1** had no effect on protein kinase C activity ( $91 \pm 3\%$ ) at concentrations as high as 10-fold above its MIC (Figure 6B). These data indicate that Pkc1 is not the direct target of the benzothioureas.

The components of the cell wall integrity pathway downstream of Pkc1 are a set of MAP kinases terminating with Mpk1 (Figure 2B). The MAP kinases of the cell wall integrity pathway are essential for the ability of *C. neoformans* to grow at  $37\text{ }^\circ\text{C}$ <sup>23</sup> but are dispensable for growth at lower temperatures. If the benzothioureas targeted MAPKs of the CWIP exclusively, then the activity of the molecules should be lost at low temperature. As shown in Figure 6C, the MIC of **1** increased from 8  $\mu\text{g}/\text{mL}$  at  $37\text{ }^\circ\text{C}$  to 16  $\mu\text{g}/\text{mL}$  at  $30\text{ }^\circ\text{C}$ , but it retained anticryptococcal activity. This is consistent with CWIP inhibition contributing to the antifungal activity of the

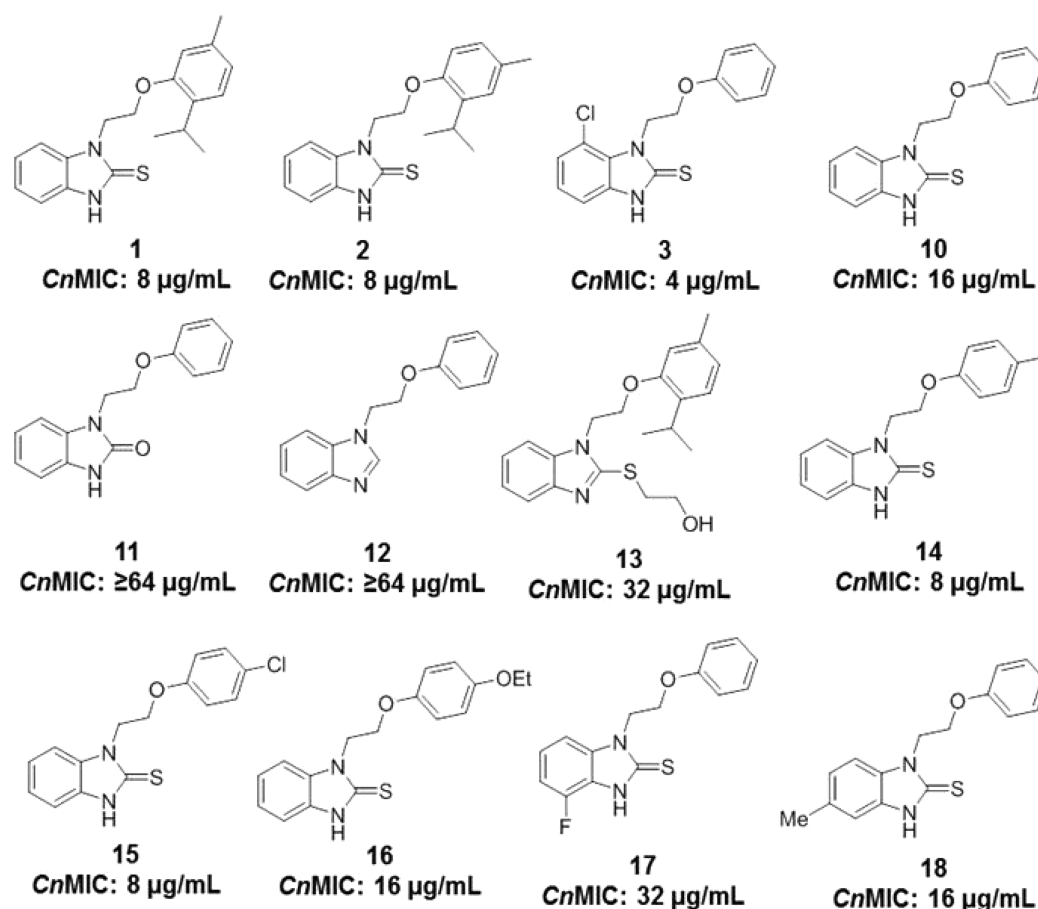


**Figure 5.** Structure–activity relationships for benzothioureas. The structure of each molecule is shown along with the minimum inhibitory concentration (MIC) against *C. neoformans* as determined by CLSI standard methods. The values are from duplicate assays.

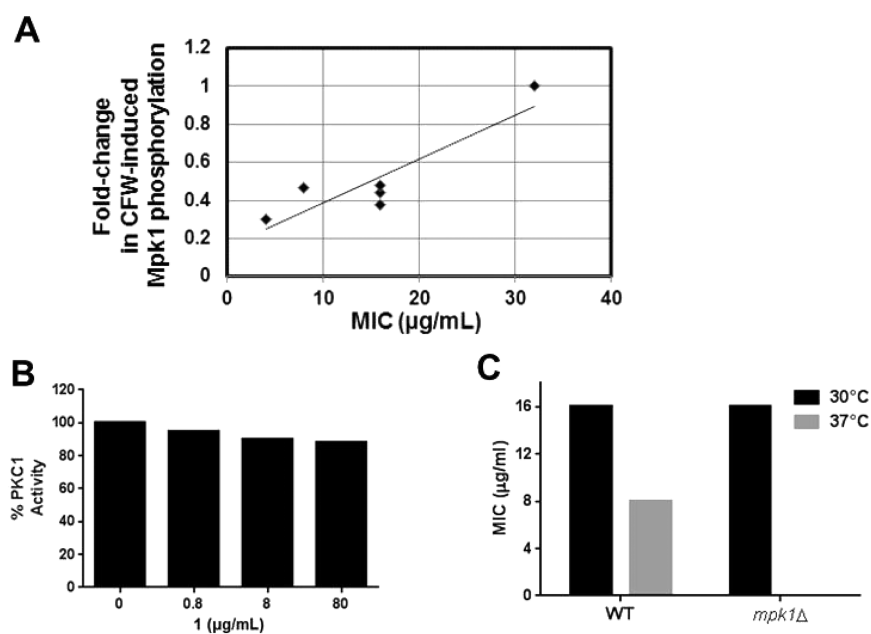


**Figure 6.** Activity of benzothioureas correlates with CWIP inhibition. (A) Plot of the MIC of benzothiourea analogues versus inhibition of Mpk1 phosphorylation. Mpk1 phosphorylation was estimated using densitometric analysis of Western blots as described under *Methods*. The MICs are from *Figure 5*. (B) Protein kinase C activity of cell lysates treated with **1** compared to DMSO-treated reactions over the range of indicated concentrations and expressed as a percentage of DMSO-treated samples. Data are means and standard deviation  $\leq 15\%$ . (C) MIC for **1** determined at 30 and 37 °C with *C. neoformans* strain CM108 and compared to the congenic *mpk1Δ* at 30 °C.

benzothioureas, but the presence of activity at 30 °C also suggests that the molecule affects other pathways as part of its mechanism of antifungal activity. Further supporting this notion, **1** is active against a *C. neoformans* strain from which *MPK1* has been deleted (Figure 6C). Because *MPK1* is essential only at mammalian body temperature,<sup>23</sup> a molecule inhibiting the MAPK cascade specifically would be expected to have no activity against *mpk1Δ*. Thus, our data indicate that the benzothioureas target processes that regulate the activity of the cell wall pathway as well as other cellular functions. The CWIP pathway receives inputs through a variety of multifunctional pathways such as phosphoinositide signaling, small G-protein activation, and other protein kinases.<sup>15,20</sup> Therefore, we suspect that the benzothioureas may be interfering with targets that mediate inputs to the CWIP as well as other functions.

In conclusion, we have identified benzothioureas as a new class of molecules that inhibit signaling through the CWIP as part of their mechanism of action. The CWIP has been validated as an antifungal drug target in *C. neoformans* on the basis of the fact that mutants lacking a functional CWIP (e.g., *mpk1Δ*) are avirulent in murine models of cryptococcosis<sup>23</sup> and undergo lysis at mammalian body temperature. Furthermore, the benzothioureas have low toxicity toward human cells and, thus, they appear to have promise for further development and optimization. Current efforts are focused on characterizing their specific molecular target.

## METHODS

### Strains, Cell Lines, Plasmids, Media, and Materials.

The primary screen was performed with *C. neoformans* var. *grubii* H99 (ATCC 208821). The MICs were determined with *C. neoformans* H99-stud (J. Heitman Laboratory collection). *C. neoformans* strain CM108 and *mpk1Δ* were obtained from the Fungal Genetics Stock Center. *C. neoformans* KN99 *MPK1-FLAG* was obtained from J. Lodge.<sup>32</sup> *S. cerevisiae* strain BY4741 (Open Biosystems) was used for all *S. cerevisiae* experiments. The reporter plasmid *RLM1-lacZ* was a gift of D. Levin.<sup>28</sup> Human cell lines HEK293 (ATCC 7740), HepG2 (ATCC 77400), HeLa (ATCC CCL-2), and A549 (ATCC; CCL-185) were used for cytotoxicity assays. Yeast media were prepared using standard recipes.<sup>29</sup> The primary screening libraries were from the Broad Institute. Commercially available molecules were obtained from Chembridge or Sigma-Aldrich and used as received.

**Representative analytical data for 1-(2-(2-isopropyl-5-methylphenoxy)ethyl)-1*H*-benzo[d]imidazole-2(3*H*)-thione (**1**):** <sup>1</sup>H NMR (300 MHz, CDCl<sub>3</sub>) δ 10.82 (d, *J* = 10.7 Hz, 1H), 7.37 (m, 1H), 7.30–7.10 (m, 3H), 7.00 (m, 1H), 6.79–6.54 (m, 2H), 4.71 (t, *J* = 4.7 Hz, 2H), 4.42 (q, *J* = 4.9 Hz, 2H), 2.97 (m, 1H), 2.27 (s, 3H), 0.93 (d, *J* = 6.1 Hz, 6H); <sup>13</sup>C NMR (125 MHz, CDCl<sub>3</sub>) δ 68.39, 155.22, 136.34, 133.90, 133.83, 130.25, 125.70, 123.37, 122.78, 121.74, 112.21, 110.08, 109.76, 65.40, 44.06, 25.96, 22.62, 21.22; HRMS (ESI+) calcd for C<sub>19</sub>H<sub>22</sub>N<sub>2</sub>OS, 327.1526 [M + H]; found, 327.1534. The synthetic methods and analytical data for all molecules are available online at <http://www.ncbi.nlm.nih.gov/pubmed/25834906>.

**Adenylate Kinase Assay.** *C. neoformans* H99 was grown overnight to midexponential phase (OD<sub>600</sub> ≤ 1) in yeast peptone 2% dextrose (YPD) medium at 30 °C, washed, and resuspended in fresh YPD (cell density = 5 × 10<sup>6</sup> cells/mL or 0.1 OD<sub>600</sub>). The inoculum (5 μL) was introduced into 1536-well plates containing molecules (7.5 nL) that had been pinned

previously. The plates were incubated at 37 °C for 4 h. ToxiLight reagent (4 μL) was added, and luminescence was measured after 30 min at room temperature using an Envision plate reader (USLum setting). For the dose–response assays, the same manipulations were carried out in 384-well plates and 100 nL of molecule suspensions was used.

**Antifungal Activity Assays.** For IC<sub>50</sub> and sorbitol suppression assays, *C. neoformans* was grown overnight in YPD at 30 °C, harvested, and inoculated into 384-well plates (30 μL; cell density: 1.5 × 10<sup>4</sup>/mL). The cells were used to inoculate plates containing a dilution series of each molecule and incubated for 24 h at 37 °C in the presence or absence of 1 M sorbitol. Alamar blue (diluted 1:10 from stock; 5 μL/well) was added to the wells, and the mixture was incubated for 2 h at 37 °C. Fluorescence was measured with an Envision Plate Reader (Ex 544 nm; Em 590 nm) for each well and compared to DMSO-treated well; IC<sub>50</sub> values were generated by curve fitting. MIC values were determined using CLSI approved methods with the 72 h end point.

**Mammalian Cell Cytotoxicity Assays.** The mammalian cell lines (Hep2G, HEK293, A549, HeLa) were exposed to a dilution series of the molecule or DMSO solvent alone for 72 h in 384-well format. Cell viability was measured using CellTiterGlo (Promega) following the manufacturer's protocol. Molecules with an LD<sub>50</sub> of <20 μM were removed from further analysis.

**Cell Wall Stress Reporter Assay.** The yeast strain CRY2[*Rlm1-lacZ*] was grown overnight in synthetic complete medium lacking uracil at 30 °C. The culture was diluted to 0.1 OD<sub>600</sub> in fresh YPD medium and grown for two doublings to 0.4 OD<sub>600</sub>. The cells were harvested, and 30 μL (cell density = 0.05 OD<sub>600</sub>) was added to 384-well plates. Solutions of molecules were added to each well by pinning (100 nL). For assays with Calcofluor white, 5 μL (40 μg/mL in water) was added to each well. The plates were incubated at room temperature for 4 h and then processed using a Gal-Screen kit (Life Technologies) using the manufacturer's protocol. Luminescence was measured with an Envision plate reader.

**Western Blot Analysis of Mpk1 Phosphorylation.** Colonies of *C. neoformans* strain H99 or *S. cerevisiae* BY4741 were picked from a freshly inoculated yeast peptone dextrose (YPD) plate and used to inoculate a 2 mL culture in liquid YPD. The culture was grown overnight in YPD at 30 °C with shaking and then diluted to an OD<sub>600</sub> = 0.2 in 25 mL of YPD. The cells were grown with shaking for 3 h and then treated with Calcofluor white (20 μg/mL), DMSO (1%), or the probe candidates (16 μg/mL final concentration, final DMSO = 1%) for 2 h. The growth rate between treated and untreated cells did not differ significantly by cell density measurements. The cells were harvested at 652g at 4 °C for 10 min. The cell pellet was resuspended in 0.3 mL of 1× lysis buffer [50 mM Tris-HCl, pH 7.5, 150 mM NaCl, 5 mM EDTA, pH 8.2, 5 mM EGTA, 0.2 mM Na<sub>3</sub>VO<sub>4</sub>, 50 mM KF, 30 mM sodium pyrophosphate, 15 mM *p*-nitrophenylphosphate, 1× protease inhibitor cocktail (Roche, 11836170001), and 10 μL/mL each of phosphatase inhibitor cocktail II and III (Sigma, P-5726 and P-0044)]. Glass beads were added to the meniscus of the suspension, and the cells were lysed by 10 cycles of bead beating (20 s) and cooling in ice (1 min). Total protein was determined using the Quick Start Bradford dye reagent (Bio-Rad), and 15 μg of total protein was loaded into precast 10% Mini-PROTEAN TGX (Bio-Rad) gels. Fractionated proteins were transferred to nitrocellulose membranes and blocked overnight at 4 °C [5%



bovine serum albumin in 50 mM Tris, pH 7.5, 150 mM NaCl, 0.05% Tween-20 (TBST)]. The membranes were probed using anti-Active MAPK (Promega, Madison, WI, USA) at 1:1000 dilution in the blocking buffer to detect phosphorylated Mpk1 followed by anti-rabbit-HRP conjugated secondary antibody (Bio-RAD, 1:10000 dilution). Blots were visualized with the ECL Plus Western blotting detection system (GE Healthcare). The blots were photographed with a GEL doc device and images processed by PhotoShop with all lanes set to identical levels/contrast/brightness. The relative density of the bands was determined using the histogram function of PhotoShop.

**Cellular Protein Kinase C Activity.** Total cellular PKC activity was measured using the PepTag Assay for Non-Radioactive Detection of Protein Kinase C kit (Promega) based on procedures previously described.<sup>25</sup> Briefly, cells were grown overnight in YPD at 30 °C with shaking. Cells were then washed three times with DPBS and adjusted to  $1 \times 10^7$  cells/mL. Whole cell lysates were prepared by glass bead lysis using the extraction buffer provided in the kit. Equivalent amounts of total cellular protein were added to each reaction, and a dilution of series of the indicated molecule was added. After 30 min of reaction time, reaction products were fractionated using agarose gel electrophoresis, visualized using a GEL DOC system, and quantified using the histogram function of Adobe PhotoShop.

## AUTHOR INFORMATION

### Corresponding Author

(D.J.K.) E-mail: [damian\\_krysan@urmc.rochester.edu](mailto:damian_krysan@urmc.rochester.edu). Phone: (585) 275-5944. Fax: (585) 273-1104.

### Notes

The authors declare no competing financial interest.

## ACKNOWLEDGMENTS

This work was supported by NIH Grants 1R01AI091422 (to D.J.K.) and, in part, 1R01AI097142 (to D.J.K.).

## REFERENCES

- (1) Brown, G. D., Denning, D. W., and Levitz, S. M. (2012) Tackling human fungal infections. *Science* 336, 647.
- (2) Perfect, J. R. (2013) Efficiently killing a sugar-coated yeast. *N. Engl. J. Med.* 368, 1354–1356.
- (3) Park, B. J., Wannemuehler, K. A., Marston, B. J., Govender, N., Pappas, P. G., and Chiller, T. M. (2009) Estimation of the current global burden of cryptococcal meningitis among persons living with HIV/AIDS. *AIDS* 23, 525–530.
- (4) Kwon-Chung, K. J., Fraser, J. A., Doering, T. L., Wang, Z., Janbon, G., Idnurm, A., and Bahn, Y. S. (2014) *Cryptococcus neoformans* and *Cryptococcus gattii*, the etiologic agents of cryptococcosis. *Cold Spring Harbor Perspect. Med.* 4, a019760.
- (5) Sloan, D. J., Dedicoat, M. J., and Lalloo, D. G. (2009) Treatment of cryptococcal meningitis in resource-limited settings. *Curr. Opin. Infect. Dis.* 22, 455–463.
- (6) Day, J. N., Chau, T. T., Wolbers, M., et al. (2013) Combination therapy for cryptococcal meningitis. *N. Engl. J. Med.* 368, 1291–1302.
- (7) Bicanic, T., Muzoora, C., Brouwer, A. E., Meintjes, G., Longley, N., Taseera, K., Rebe, K., Loyse, A., Jarvis, J., Bekker, L. G., Wood, R., Limmathurostakul, D., Chierakul, W., Stepniewska, K., White, N. J., Jaffar, S., and Harrison, T. S. (2009) Independent association of clearance of infection and clinical outcome of HIV-associated cryptococcal meningitis: analysis of combined cohort of 262 patients. *Clin. Infect. Dis.* 49, 702–709.
- (8) Roemer, T., and Krysan, D. J. (2014) Antifungal drug development: challenges, unmet clinical needs, and new approaches. *Cold Spring Harbor Perspect. Med.* 1, a019703.

(9) DiDone, L., Scrimale, T., Baxter, B. K., and Krysan, D. J. (2010) A high-throughput assay of yeast cell lysis for drug discovery and genetic analysis. *Nat. Protoc.* 5, 1107–1114.

(10) Dehdashti, S. J., Abbott, J., Nguyen, D. T., McKew, J. C., Williamson, P. R., and Zheng, W. (2013) A high-throughput screening assay for assessing the viability of *Cryptococcus neoformans* under nutrient starvation conditions. *Anal. Bioanal. Chem.* 405, 6823–6829.

(11) Rabjohns, J. L., Park, Y. D., Dehdashti, J., Sun, W., Henderson, C., Zelazny, A., Metallo, S. J., Zheng, W., and Williamson, P. R. (2014) A high-throughput screening assay for fungicidal compounds against *Cryptococcus neoformans*. *J. Biomol. Screen.* 19, 270–277.

(12) Butts, A., and Krysan, D. J. (2012) Antifungal drug discovery: something old and something new. *PLoS Pathog.* 8, e1002870.

(13) Maligie, M. A., and Selitrennikoff, C. P. (2005) *Cryptococcus neoformans* resistance to echinocandins: (1,3)- $\beta$ -glucan synthase activity is sensitive to echinocandins. *Antimicrob. Agents Chemother.* 49, 2851–6.

(14) Li, R. K., and Rinaldi, M. G. (1999) In vitro antifungal activity of nikkomycin Z in combination with fluconazole or itraconazole. *Antimicrob. Agents Chemother.* 43, 1401–1405.

(15) Doering, T. L. (2009) How sweet it is! Cell wall biogenesis and polysaccharide capsule formation in *Cryptococcus neoformans*. *Annu. Rev. Microbiol.* 63, 223–247.

(16) Butts, A., DiDone, L., Koselny, K., Baxter, B. K., Chabrier-Rosello, Y., Wellington, M., and Krysan, D. J. (2013) A re-purposing approach identifies off-patent drugs with fungicidal cryptococcal activity, a common structural chemotype, and pharmacological properties relevant to the treatment of cryptococcosis. *Eukaryotic Cell* 12, 278–287.

(17) Farrer, R. A., Desjardins, C. A., Sakthikumar, S., Gujja, S., Saif, S., Zeng, Q., Chen, Y., Voelz, K., Heitman, J., May, R. C., Fisher, M. C., and Cuomo, C. A. (2015) Genome evolution and innovation across the four major lineages of *Cryptococcus gattii*. *mBio* 6, e00868-15.

(18) Brown, J. C., Nelson, J., VanderSluis, B., Deshpande, R., Butts, A., Kagan, S., Polacheck, I., Krysan, D. J., Myers, C. L., and Madhani, H. D. (2014) Unraveling the biology of a fungal meningitis pathogen using chemical genetics. *Cell* 159, 1168–87.

(19) Philips, J., and Herskowitz, I. (1997) Osmotic balance regulates cell fusion during mating in *Saccharomyces cerevisiae*. *J. Cell Biol.* 138, 961–974.

(20) Levin, D. E. (2011) Regulation of cell wall biogenesis in *Saccharomyces cerevisiae*: the cell wall integrity signaling pathway. *Genetics* 189, 1145–1168.

(21) Hartland, C. L., Pu, J., Krysan, D., DiDone, L., Moquist, P. N., Dandapani, S., Munoz, B., Palmer, M., and Schreiber, S. (2014) Discovery and evaluation of fungicidal anti-cryptococcal molecules. *Probe Reports from the NIH Molecular Libraries Program* [Internet], National Center for Biotechnology Information (US), Bethesda, MD, USA, 2010–2014 Apr 15 (updated 2015 Jan 16).

(22) Krysan, D. J., and DiDone, L. (2008) A high-throughput screening assay for small molecules that disrupt yeast cell integrity. *J. Biomol. Screening* 13, 657–64.

(23) Kraus, P. R., Fox, D. S., Cox, G. M., and Heitman, J. (2003) The *Cryptococcus neoformans* MAP kinase Mpk1 regulates cell integrity in response to antifungal drugs and loss of calcineurin function. *Mol. Microbiol.* 48, 1377–1387.

(24) Bahn, Y. S., Kojima, K., Cox, G. M., and Heitman, J. (2005) Specialization of the HOG pathway and its impact on differentiation and virulence in *Cryptococcus neoformans*. *Mol. Biol. Cell* 16, 2285–2300.

(25) Baxter, B. K., DiDone, L., Oga, D., Schor, S., and Krysan, D. J. (2011) Identification, in vitro activity and mode of action of phosphoinositide-1 kinase inhibitors as antifungal molecules. *ACS Chem. Biol.* 6, 502–510.

(26) National Committee for Clinical Laboratory Standards. (2002) *Reference Method for Broth Dilution Antifungal Susceptibility Testing of Yeasts. Approved Standard M27-A2*, National Committee for Clinical Laboratory Standards, Wayne, PA, USA.

(27) Madden, K., Sheu, Y. J., Baetz, K., Andrews, B., and Snyder, M. (1997) SBF regulator as a target of yeast PKC-MAP kinase pathway. *Science* 275, 1781–1784.

(28) Jung, U. S., Sobering, A. K., Romeo, M. J., and Levin, D. E. (2002) Regulation of Rlm1 transcription factor by the Mpk1 cell wall integrity MAP kinase. *Mol. Microbiol.* 46, 781–789.

(29) Chabrier-Rosello, Y., Gerik, K., Koselny, K., DiDone, L., Lodge, J. K., and Krysan, D. J. (2013) *Cryptococcus neoformans* phosphoinositide-dependent kinase 1 (PDK1) ortholog is required for stress tolerance. *Eukaryotic Cell* 12, 12–22.

(30) Markovich, S., Yekutieli, A., Shalit, J., Shadkchan, V., and Osherov, N. (2004) Genomic approach to identification of mutations affecting caspofungin susceptibility in *Saccharomyces cerevisiae*. *Antimicrob. Agents Chemother.* 48, 3871–3876.

(31) Durant, G. J., Emmett, J. C., Ganellin, C. R., Miles, P. D., Parsons, M. E., Prain, H. D., and White, G. R. (1977) Cyanoguanidine-thiourea equivalence in the development of histamine H<sub>2</sub>-receptor antagonist, Cimetidine. *J. Med. Chem.* 20, 901–966.

(32) Gerik, K. J., Bhimireddy, S. R., Ryerse, J. S., Specht, C. A., and Lodge, J.K. (2008) Pkc1 is essential for protection against both oxidative and nitrosative stresses, cell integrity, and normal manifestation of virulence factors in the pathogenic fungus *Cryptococcus neoformans*. *Eukaryotic Cell* 7, 1685–1698.